AGU PUBLICATIONS

Geochemistry, Geophysics, Geosystems

RESEARCH ARTICLE
10.1002/2014GC005629

Special Section:
Studies of Seamount Trails: Implications for Geodynamic Mantle Flow Models and the Geochemical Evolution of Primary Hotspots

Re-Os isotope and platinum group elements of a FOcal ZOne mantle source, Louisville Seamounts Chain, Pacific ocean

Maria Luisa G. Tejada[1,3], Takeshi Hanyu[1], Akira Ishikawa[1,2], Ryoko Senda[1], Katsuhiko Suzuki[3], Godfrey Fitton[4], and Rebecca Williams[5]

[1]Department of Solid Earth Geochemistry, Japan Agency for Marine-Earth Science and Technology, Yokosuka, Japan, [2]Department of Earth Science and Astronomy, University of Tokyo, Tokyo, Japan, [3]Research and Development Center for Submarine Resources, Japan Agency for Marine-Earth Science and Technology, Yokosuka, Japan, [4]School of Geosciences, Grant Institute, University of Edinburgh, UK, [5]Department of Geography, Environment and Earth Sciences, University of Hull, UK

Key Points:
- The LSC mantle source has a small range of mantle-like ($^{187}Os/^{188}Os)_i$
- The Os isotopes and PGE contents suggest little or no recycled components
- The PGE variations are best explained by sulfide-present low-degree melting

Correspondence to:
M. L. G. Tejada,
mtejada@jamstec.go.jp

Citation:
Tejada, M. L. G., T. Hanyu, A. Ishikawa, R. Senda, K. Suzuki, G. Fitton, and R. Williams (2015), Re-Os isotope and platinum group elements of a FOcal ZOne mantle source, Louisville Seamounts Chain, Pacific ocean, *Geochem. Geophys. Geosyst.*, *16*, 486–504, doi:10.1002/2014GC005629.

Received 23 OCT 2014
Accepted 27 JAN 2015
Accepted article online 3 FEB 2015
Published online 19 FEB 2015

Abstract The Louisville Seamount Chain (LSC) is, besides the Hawaiian-Emperor Chain, one of the longest-lived hotspot traces. We report here the first Re-Os isotope and platinum group element (PGE) data for Canopus, Rigil, and Burton Guyots along the chain, which were drilled during IODP Expedition 330. The LSC basalts possess $(^{187}Os/^{188}Os)_i = 0.1245–0.1314$ that are remarkably homogeneous and do not vary with age. A Re-Os isochron age of 64.9 ± 3.2 Ma was obtained for Burton seamount (the youngest of the three seamounts drilled), consistent with ^{40}Ar-^{39}Ar data. Isochron-derived initial $^{187}Os/^{188}Os$ ratio of 0.1272 ± 0.0008, together with data for olivines (0.1271–0.1275), are within the estimated primitive mantle values. This $(^{187}Os/^{188}Os)_i$ range is similar to those of Rarotonga (0.124–0.139) and Samoan shield (0.1276–0.1313) basalts and lower than those of Cook-Austral (0.136–0.155) and Hawaiian shield (0.1283–0.1578) basalts, suggesting little or no recycled component in the LSC mantle source. The PGE data of LSC basalts are distinct from those of oceanic lower crust. Variation in PGE patterns can be largely explained by different low degrees of melting under sulfide-saturated conditions of the same relatively fertile mantle source, consistent with their primitive mantle-like Os and primordial Ne isotope signatures. The PGE patterns and the low $^{187}Os/^{188}Os$ composition of LSC basalts contrast with those of Ontong Java Plateau (OJP) tholeiites. We conclude that the Re-Os isotope and PGE composition of LSC basalts reflect a relatively pure deep-sourced common mantle sampled by some ocean island basalts but is not discernible in the composition of OJP tholeiites.

1. Introduction

The Louisville Seamount Chain (LSC) is recognized as a product of one of the few primary Pacific hotspots, together with Hawaii and Easter [*Courtillot et al*., 2003], based on its linear morphology and its long-lived age-progressive volcanism [*Koppers et al*., 2004, 2011]. This volcanic chain is thought to have formed as the Pacific plate moved over a persistent mantle-melting anomaly or hotspot in the past 80 Myr [*Cheng et al*., 1987]. Available data obtained from dredged rocks define a limited range in isotopic composition [*Cheng et al*., 1987; *Hawkins et al*., 1987; *Beier et al*., 2011; *Vanderkluysen et al*., 2014], suggesting that the mantle source has been remarkably homogeneous for the whole ~80 Myr duration of magmatic activity. These data contrast strongly with those obtained from the Hawaiian-Emperor Seamount Chain, which indicate a heterogeneous mantle source expressed in the compositional differences among and within volcanoes. However, compared to the Hawaiian-Emperor Chain volcanoes, those belonging to the LSC have been barely studied.

Five of the older guyots along the LSC were drilled during the Integrated Ocean Drilling Program (IODP) Expedition 330 from December 2010 to February 2011 (Figure 1). One of the objectives of the expedition is to better understand the eruptive cycle and geochemical evolution of typical Louisville volcanoes. Previous dredging recovered mostly alkalic basalts, basanites, and tephrites [*Hawkins et al*., 1987; *Beier et al*., 2011; *Vanderkluysen et al*., 2014], which raises the question of whether or not the Louisville volcanoes were constructed solely by alkalic shield volcanism. The other point of interest is the nature of the source, which up until now has had very limited support for a deep-rooted mantle [e.g., *Hanyu*, 2014] with little influence

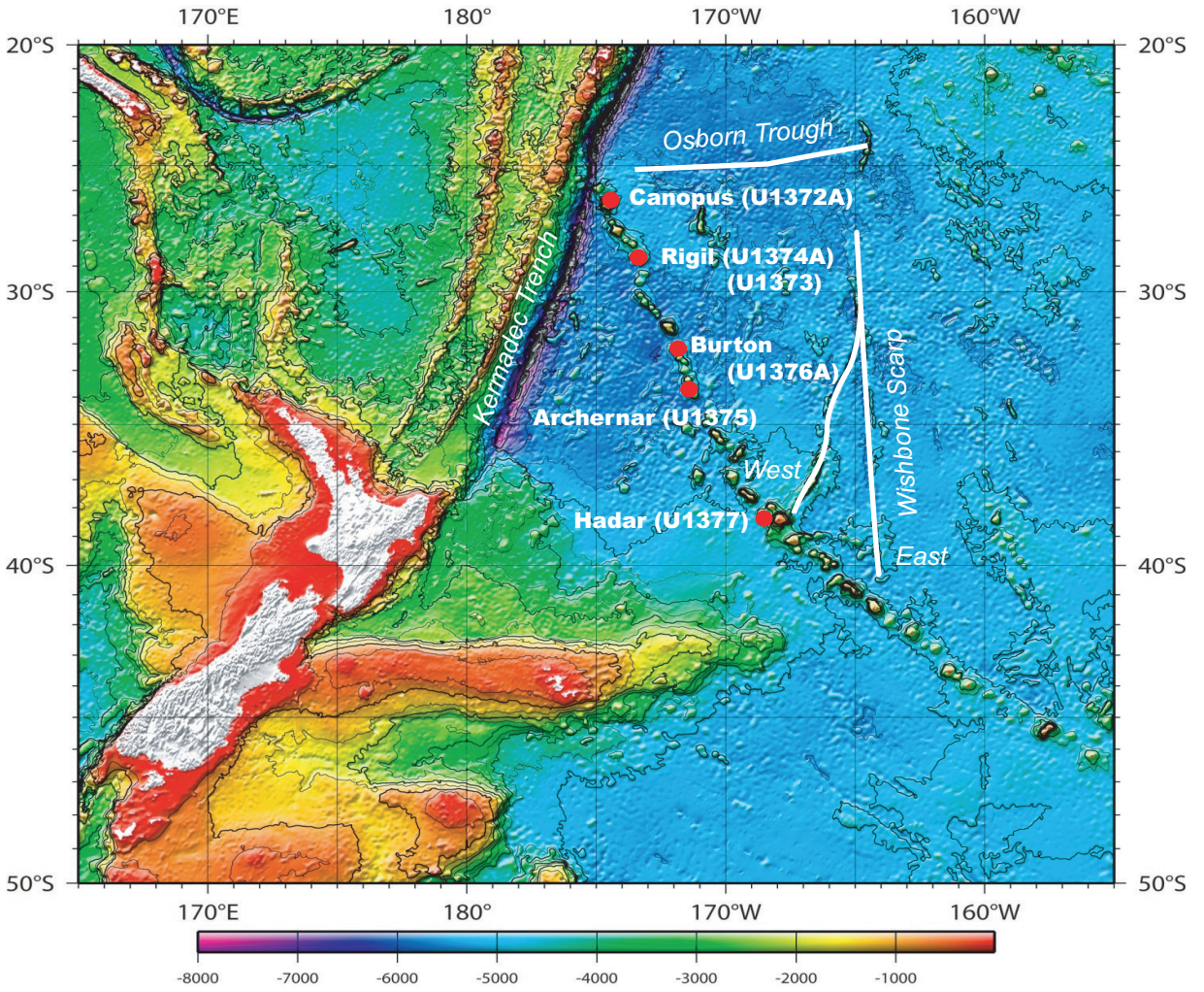

Figure 1. Louisville Seamount Chain showing the sites and seamounts drilled during the IODP Expedition 330 [*Expedition 330 Scientists*, 2011]. Structural features around the seamounts, such as the Wishbone Scarps, Osborn Trough, and Kermadec Trench are also shown for reference.

from heterogeneities found in most ocean island basalts (OIB). For example, isotopic and trace element data suggest a long-lived and remarkably homogeneous mantle source quite distinct from that of mid-ocean ridge basalts (MORB) [*Cheng et al*., 1987; *Hawkins et al*., 1987; *Beier et al*., 2011; *Vanderkluysen et al*., 2014] and, combined with the age-progressive volcanism [*Koppers et al*., 2004, 2011], led these workers to suggest a source with an affinity to the FOcal ZOne (FOZO) [*Hart et al*., 1992] mantle inferred to represent a common component in the source of OIBs. Finally, Expedition 330 was expected to shed further light on the inferred link with the Ontong Java Plateau (OJP) emplacement as the potential plume-head stage of the Louisville hotspot development.

The present study aims to characterize the mantle source of the LSC in terms of the Re-Os isotope and platinum-group element (PGE) abundances and to examine the temporal geochemical variation along the seamount chain. We show that the Os isotopic data for the LSC basalts also fall within a limited range very close to estimated primitive mantle composition (also termed as "primitive upper mantle," PUM) [*Meisel et al*., 2001] and that the differences in PGE abundances among seamounts may be explained by a range of low-degree melt extraction under sulfide-saturated condition from a relatively fertile mantle with little or no contribution from recycled crust. Together with their primordial Ne isotopic signature [*Hanyu*, 2014], these results support a deeply rooted mantle source for the LSC.

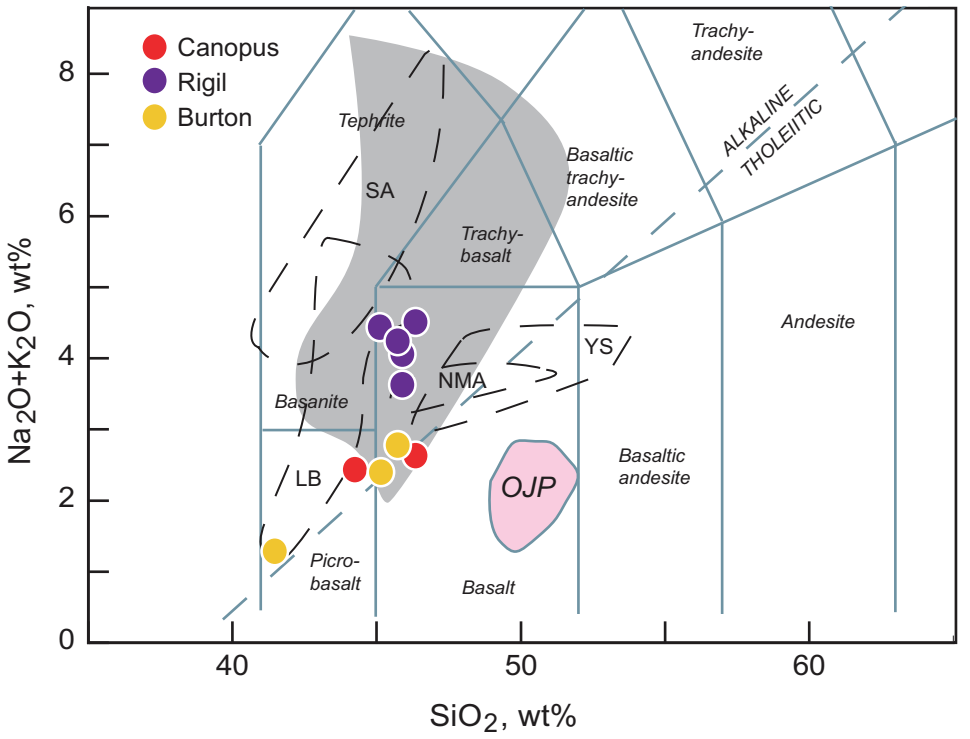

Figure 2. Total alkali versus SiO_2 plot for LSC basalts analyzed for Os isotopes and Re and platinum group element (PGE) abundances showing the slightly different composition of samples from Rigil seamount. Also shown are data fields for the dredged samples from Louisville seamounts [*Cheng et al.*, 1987; *Hawkins et al.*, 1987; *Beier et al.*, 2011; *Vanderkluysen et al.*, 2014], Ontong Java Plateau (OJP) tholeiites [*Fitton and Godard*, 2004], and the associated alkalic rocks from the Solomon Islands (YS = Younger Series, NMA = North Malaita Alkalics, SA = Sigana Alkalics) [*Tejada et al.*, 1996], and Lyra Basin (LB) [*Tejada et al.*, 2015] for reference.

2. Geological Background and Samples

Recent IODP Expedition 330 recovered in situ volcanic rocks from four of the five drilled seamounts that range in age from 50 to 74 Ma (Figure 1): Canopus (Site U1372, 74.2 ± 0.5 Ma); Rigil (Sites U1373, 69.5±0.4 Ma and U1374, 70.7±0.6 Ma); Burton (Site U1376, 64.1 ± 0.5 Ma); Achernar (Site U1375, 58.5 Ma); and Hadar (Site U1377, 50 ± 0.3 Ma) [*Expedition 330 Scientists*, 2011; *Koppers et al.*, 2012a, 2012b]. Before this expedition, information on the composition and geochemistry, as well as the age of the LSC was exclusively based on data obtained from dredged volcanic rocks [*Cheng et al.*, 1987; *Hawkins et al.*, 1987; *Lonsdale*, 1988; *Watts et al.*, 1988; *Beier et al.*, 2011; *Koppers et al.*, 2004, 2011]. Dredged samples included lava flows and pillow basalt fragments that are silica-undersaturated and have trace element abundances and radiogenic isotopic compositions typical of OIBs. On the other hand, except at Achernar Seamount, drilling recovered lava flows, pillow basalts, dikes, scoriaceous and blocky breccias, and peperites, indicating a change in eruption environment from submarine to subaerial. Compared to dredged rocks, the drilled samples have a similar or comparable geochemical composition but display a smaller variability, especially in relatively mobile major elements, reflecting their less altered state [*Expedition 330 Scientists*, 2011]. They range from transitional to alkalic basalts that differ slightly in trace element abundances (Figures 2 and 3). None of the drill holes encountered a tholeiitic basement.

Ten samples, with variable range in MgO contents from 5.86 to 21.69 wt %, were selected from Canopus (U1372), Rigil (U1374), and Burton (U1376) seamounts (Figure 1) for Os isotope and PGE analyses in order to investigate the temporal and fractionation variation with Os isotopic composition and PGE abundances (Tables 1 and 2). Samples from both Canopus and Burton seamounts are transitional basalts, while those from Rigil seamount are alkali basalts (Figure 2). Two of the four samples with <8 wt % MgO (U1374A-70R-1, 56–59 cm and U1374A-52R-2, 96–99 cm) are aphyric. Most of the high-MgO basalt samples (9–22 wt % MgO, Table 1, Figure 3) are moderately to highly olivine-phyric and contain olivine phenocrysts that are fresh and range in size from 1 to 3 mm. One of the Burton seamount samples, U1376A-21R-5, 0–16 cm,

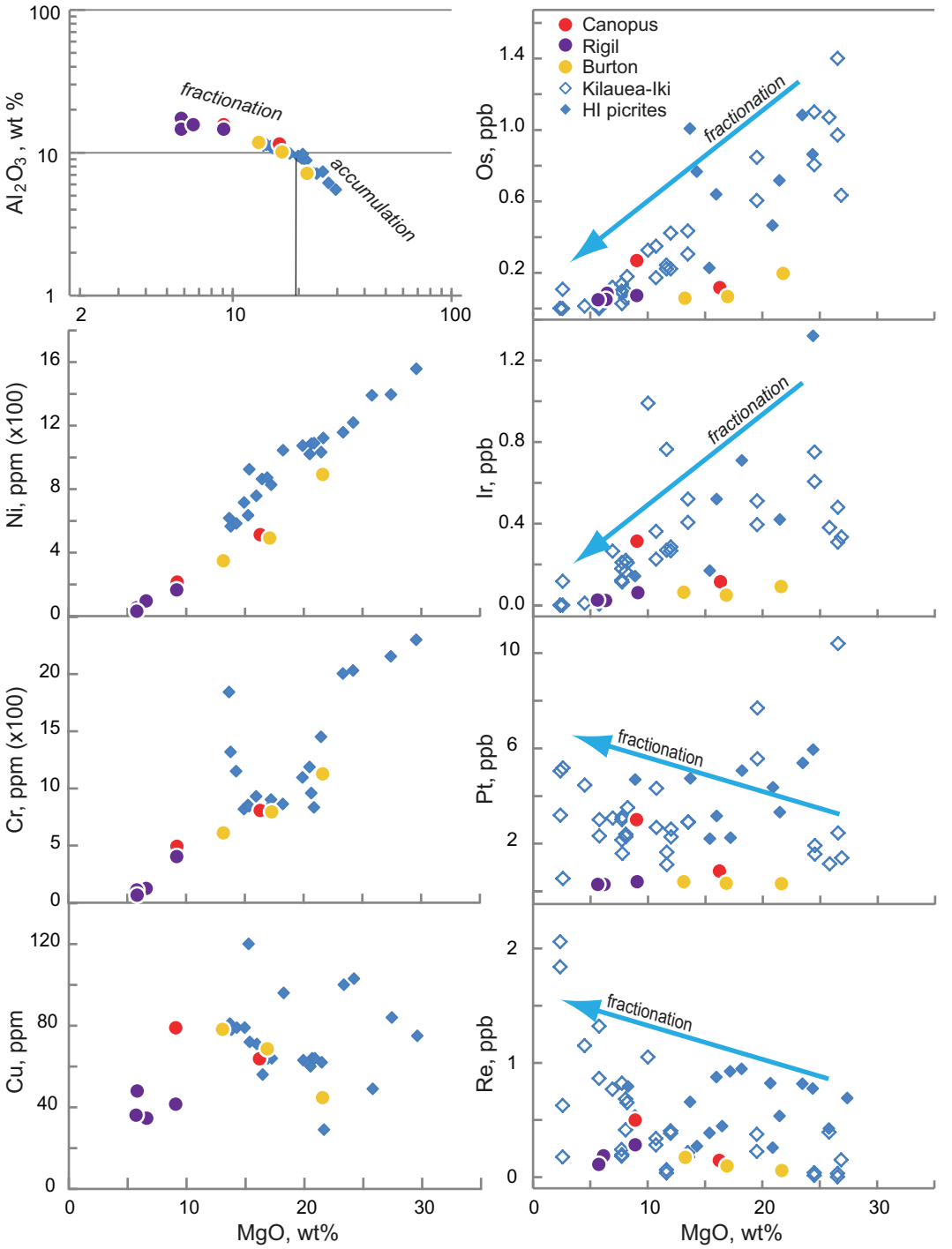

Figure 3. MgO versus Al_2O_3, Ni, Cr, Cu, and PGE abundance in LSC basalts compared with those of Kilauea Iki lavas in Hawaii [*Pitcher et al.*, 2009] and Hawaiian (HI) picrites [*Norman and Garcia*, 1999; *Bennett et al.*, 2000]. Olivine fractionation versus accumulation trends for Hawaiian picrites based on MgO versus Al_2O_3 plot [*Norman and Garcia*, 1999] are shown for comparison. The Kilauea Iki data demonstrate the PGE variation with increasing crystallization. The PGE data of the LSC basalts do not vary with crystallization and are lower than those of the Kiluea Iki data especially at higher MgO contents, except for Pt and Pd in one sample from Canopus seamount.

contains clusters of olivine phenocrysts which have been accumulated through crystal settling, based on its Al_2O_3 and MgO contents that are the lowest and highest, respectively, among our samples (Figure 3). Olivine mineral separates from this olivine-enriched sample and another highly phyric one, U1376A-8R-6, 122–128 cm, were also analyzed to derive the primary magmatic $^{187}Os/^{188}Os$ composition. Previous studies have

Table 1. Platinum Group Element Concentrations With Selected Major and Trace Element Compositions for Louisville Core Samples[a]

IODP Sample ID	MgO (wt %)	Al_2O_3 (wt %)	Ni (ppm)	Cr (ppm)	Cu (ppm)	Ir (ppb)	2σ	Ru (ppb)	2σ	Pt (ppb)	2σ	Pd (ppb)	2σ
U1372A-9R-6, 12–17 cm (0–15 cm)	16.29	11.33	512.9	803.9	63.6	0.1114	0.0025	0.4165	0.0061	0.785	0.011	0.551	0.016
U1372A-38R-3, 86–92 cm (96–99 cm)	9.09	14.96	175.6	481.3	79.3	0.3077	0.0062	0.1845	0.0036	3.034	0.043	2.501	0.040
U1374A-3R-3, 11–14 cm (3R-2, 126–137 cm)	9.11	14.71	191.7	442.1	41.6	0.0423	0.0010	0.0653	0.0014	0.300	0.007	0.207	0.008
U1374A-32R-3, 128–135 cm (105–108 cm)	6.51	15.93	78.8	101.0	35.4	*0.0025*	*0.0004*	*0.0065*	*0.0008*	*0.057*	*0.005*		
U1374A-37R-3, 39–44 cm (36R-1, 62–68 cm)	6.54	15.88	94	120.2	34.1	*0.0031*	*0.0004*	*0.0042*	*0.0008*	*0.069*	*0.005*		
U1374A-52R-2, 78–83 cm (96–99 cm)	5.87	14.67	39.9	26.5	48.4	*0.0012*	*0.0001*						
U1374A-70R-1, 60–65 cm (56–59 cm)	5.86	16.72	33.7	16.0	36.0	*0.0011*	*0.0001*						
U1376A-8R-5, 111–116 cm (8R-6, 122–128 cm)	16.87	10.18	498.7	808.1	69.2	0.0328	0.0012	0.1270	0.0025	0.179	0.011	0.151	0.008
U1376A-14R-3, 3–8 cm (14R-2, 94–97 cm)	13.15	11.69	349.5	609.6	77.8	0.0426	0.0015	0.1300	0.0026	0.377	0.012	0.204	0.009
U1376A-21R-5, 17–22 cm (0–16 cm)	21.69	7.10	888	1131.8	43.9	0.0854	0.0018	0.5340	0.0099	0.266	0.006	0.168	0.008
Blank						0.0034		0.0102		0.157		0.100	
Standard													
BIR-1a, measured						0.1320	0.0003	0.4981	0.0008	4.208	0.005	5.803	0.010
Published[b]						0.149	0.031	0.278	0.067	4.30	0.22	6.11	0.24
Published[c]						0.143	0.007	0.519	0.011	4.37	0.22	5.84	0.09

[a]Notes: Numbers in italics are below or very close to blank values. Numbers in parentheses are sample intervals used for Os isotope and PGE analyses; 2σ = 2 sigma error.
[b]*Meisel and Moser* [2004].
[c]*Ishikawa et al.* [2014].

shown that early crystallizing olivine may be shielded from the effect of later crustal assimilation, especially in low-Os basalts [*Jackson and Shirey*, 2011; *Hanyu et al*., 2011]. The Forsterite (Fo) values in olivine cores of Louisville basalts range from 78 to 90, with up to 0.4 wt % NiO, suggesting that olivines are phenocrysts in equilibrium with the magmas or have been derived from previous magmas with similar compositions (S.

Table 2. Re-Os Isotope and Re and Os Concentration Data for Louisville Core Samples[a]

Sample No.	Seamount	Age (Ma)	Re (ppt)	2σ	Os (ppt)	2σ	$^{187}Os/^{188}Os$	2σ	$^{187}Re/^{188}Os$	2σ	$(^{187}Os/^{188}Os)_t$
Whole rock											
U1372A-9R-6, 0–15 cm	Canopus	74	122	8	106	0.2	0.1345	0.0003	5.53	0.36	0.1274
U1372A-38R-3, 96–99cm	Canopus	74	271	14	270	0.5	0.1335	0.0002	4.84	0.24	0.1273
U1374A-3R-2, 126–127 cm	Rigil	71	499	24	72	0.2	0.1672	0.0009	33.6	1.6	0.1263
U1374A-32R-3, 105–108cm	Rigil	71	179	10	8.99	0.03	0.2431	0.0010	97.5	5.7	0.1245
U1374A-36R-1, 62–68 cm	Rigil	71	127	9	8.58	0.02	0.2191	0.0013	72.0	5.3	0.1314
U1374A-52R-2, 96–99 cm	Rigil	71	356	6	10	0.5					
U1374A-70R-1, 56–59 cm	Rigil	71	347	6							
U1376A-8R-6, 122–128 cm	Burton	64	91	1	26	0.2	0.1460	0.0014	17.2	0.5	0.1274
U1376A-14R-2, 94–97 cm	Burton	64	176	8	43	0.1	0.1488	0.0004	20.0	0.5	0.1272
U1376A-21R-5, 0–16 cm	Burton	64	51	1	187	0.7	0.1267	0.0003	1.31	0.03	0.1253
WR blank			0.65		0.57	0.01	0.2073	0.0104			
Standard											
BIR-1a			681	17	336	0.7	0.1336	0.0005	9.80	0.3	
Published[b]			634	28	374	46	0.1400	0.0080	8.28	1.0	
Published[c]			684	5	345	24	0.1330	0.0007	9.62	0.64	
Olivine											
U1376A-8R-6, cm	Burton		*b.b.*		231	2	0.1275	0.0016			
Duplicate			*b.b.*		231	2	0.1271	0.0010			
U1376A-21R-5, cm	Burton		*b.b.*		13	0.2	0.1272	0.0066			
OL blank			1.6		0.27	0.01	0.2204	0.0094			

[a]Notes: b.b. = below background values; 2σ = 2 sigma error.
[b]*Meisel and Moser* [2004] by HPA.
[c]*Ishikawa et al.* [2014] by ID-ICPMS.

Machida, personal communication, 2014). Thus, these olivine phenocrysts can be used to determine the original magmatic Os isotopic compositions and that of the LSC source. Osmium isotopes and Re and PGE abundances were determined for two whole-rock and olivine pairs from Site U1376A for comparison (Table 2).

3. Methods

Sample preparation and X-ray Fluorescence analysis for major and trace elements used in this study were carried out at the University of Edinburgh on a Philips PW2404 automatic X-ray spectrometer. The techniques used are essentially similar to those described by *Fitton et al*. [1998], with modifications noted by *Fitton and Godard* [2004]. Analytical precision and accuracy are comparable to the values reported by *Fitton et al*. [1998].

For Re-Os isotope and PGE analyses, the whole rock samples taken from adjacent core intervals to those analyzed for major and trace elements (Table 1) were cleaned of drilling and cutting marks by polishing off the surfaces prior to sequential ultrasonic cleaning of samples in distilled water, deionized ultrapure water, and acetone. The samples were dried in an oven overnight before they were further processed. They were then wrapped in thick paper and crushed into ~3 mm fragments using a steel mortar and pestle. Only alteration-free and interior fragments (as much as possible) were picked under a hand lens, in order to avoid alteration minerals in veins and amygdules and potential contamination introduced from drilling, polishing, and crushing. The handpicked fragments were ground in an alumina mill and then both Os isotopes and PGE and Re abundances were measured from the same rock powder digestion.

One to 1.5 g of unleached whole-rock powders were weighed, combined with Re and PGE spikes, and sealed in Carius tubes with 2.5 mL of 9 *M* HCl and 7.5 mL of 16 *M* HNO_3. Digestion of samples was carried out at 240°C for 72 h in order for spike and sample to equilibriate [*Ishikawa et al*., 2014], after which Os was separated by solvent extraction followed by microdistillation [*Cohen and Waters*, 1996; *Roy-Barman and Allegre*, 1995]. The extraction residues were then dried and further digested in teflon beakers by HF addition (desilicification) to improve recovery of Re and PGEs from the samples [*Dale et al*., 2012; *Ishikawa et al*., 2014]. The PGE and Re were purified by a three-step separation method described in *Ishikawa et al*. [2014], which includes anion and cation exchange column extraction [*Shinotsuka and Suzuki*, 2007]. Osmium was measured as oxide by thermal ionization mass spectrometry (TIMS) in negative ion mode, and Re and PGE concentrations were determined by isotope dilution inductively-coupled-plasma mass spectrometry (ID-ICPMS) at Japan Agency for Marine-Earth Science and Technology (JAMSTEC). Analytical procedures of both TIMS and ICP-MS followed those described by *Ishikawa et al*. [2014]. Blank contributions are negligible (<1%) for Re and for Os, except for samples with low Os concentration (<10 ppt), where it is less than 7%. Total procedure blanks and measurement results for BIR-1a standard are presented with data in Tables 1 and 2.

Olivine grains were separated from crushed whole rocks by handpicking under a binocular microscope to remove altered parts and contaminants. They were cleaned in an ultrasonic bath with diluted HCl, HNO_3, and ultrapure deionized water, successively, for 5 min and rinsed with ultrapure water in between. After drying in an oven, they were ground by hand in an agate mortar. Olivine powders (25–300 mg) were weighed, combined with PGE and Re spikes, and digested with 1 mL of 9 *M* HCl and 3 mL of 16 *M* HNO_3 in a sealed Carius tube at 240°C for 72 h. Osmium separation and isotopic measurement, as well as Re and PGE purification and abundance determination, procedures are similar to those applied for the whole rocks, except for the lesser amount of reagents (half of that for whole rocks) used for Os extraction. Os blank contribution is $\leq$ 2% for the olivine samples.

4. Results

4.1. Re-Os Isotopes

Whole rock Os isotope data (Table 2) show that the high-MgO samples with >8 wt % MgO from Canopus and Burton seamounts generally have lower measured $^{187}Os/^{188}Os$ values of 0.1267–0.1488. In contrast, the Rigil seamount samples with lower (<8 wt %) MgO contents and much higher abundances of Re relative to Os also have higher present-day $^{187}Os/^{188}Os$ values of 0.1672–0.2431. These results are consistent with

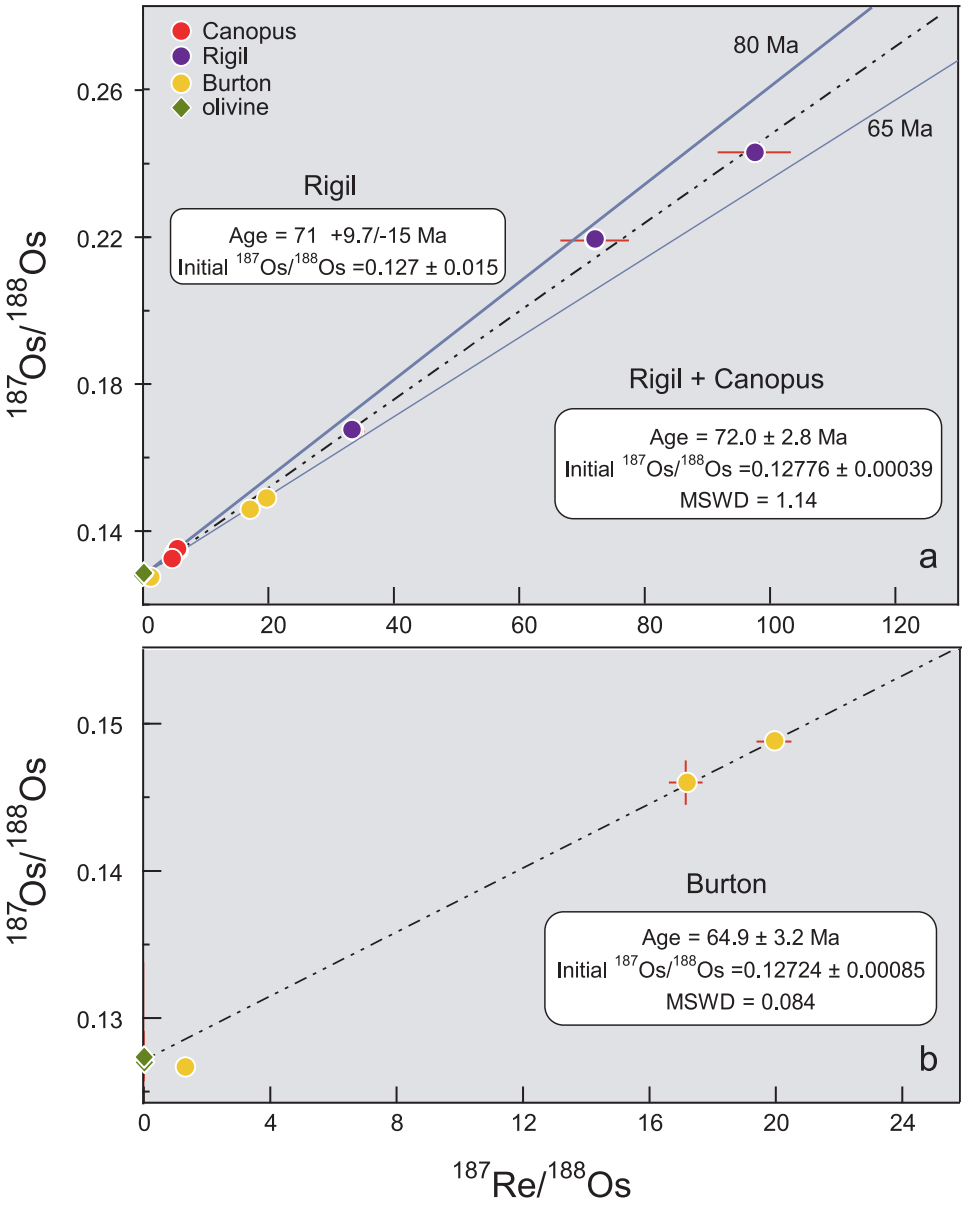

Figure 4. (a) Comparison of LSC Re-Os data with 80, 72, and 65 Ma isochrons, showing the limited scatter that can be attributed to alteration effects. The isochrons are inferred from available ^{40}Ar-^{39}Ar dates [*Koppers et al.*, 2004, 2011, 2012a, 2012b]. The dashed line is the apparent 72 Ma Re-Os isochron for Canopus and Rigil seamounts whole rock data with age and initial ^{187}Os/^{188}Os ratios indicated. Also shown, for comparison, is the age and initial ratios for Rigil seamount whole rock data if robust regression model is used to calculate the isochron [*Ludwig*, 2003]. (b) Re-Os isochron plot for Burton seamount whole rock and olivine data (except for U1376A-21R-5, 0–16 cm that may have been affected by Re addition) with an age that is in excellent agreement with published ^{40}Ar-^{39}Ar age (64.1 ± 0.5 Ma) [*Koppers et al.*, 2012b] and an initial ^{187}Os/^{188}Os ratio that is identical to values derived from olivine separates. Isochron plots were derived by Isoplot [*Ludwig*, 2003]. Most of the errors are smaller or the same size as the symbols.

radiogenic growth from the same mantle source as indicated by the plot of ^{187}Re/^{188}Os versus ^{187}Os/^{188}Os, which show the expected evolution growth lines or isochrons given their ages of 64–74 Ma, based on available ^{40}Ar-^{39}Ar data [*Koppers et al.*, 2004, 2011, 2012b] (Figure 4a). Note that there is no significant deviation from the isochrons, suggesting the reliability of the results. Some scatter in the data may be attributable to possible Re loss or addition (points displaced left and right of the isochron, respectively) during submarine alteration.

Age correction gives a limited range in initial ^{187}Os/^{188}Os values of 0.1245–0.1314, which are remarkably unradiogenic compared to most Pacific OIB data (Figure 5). For comparison, ^{187}Os/^{188}Os data for Pacific

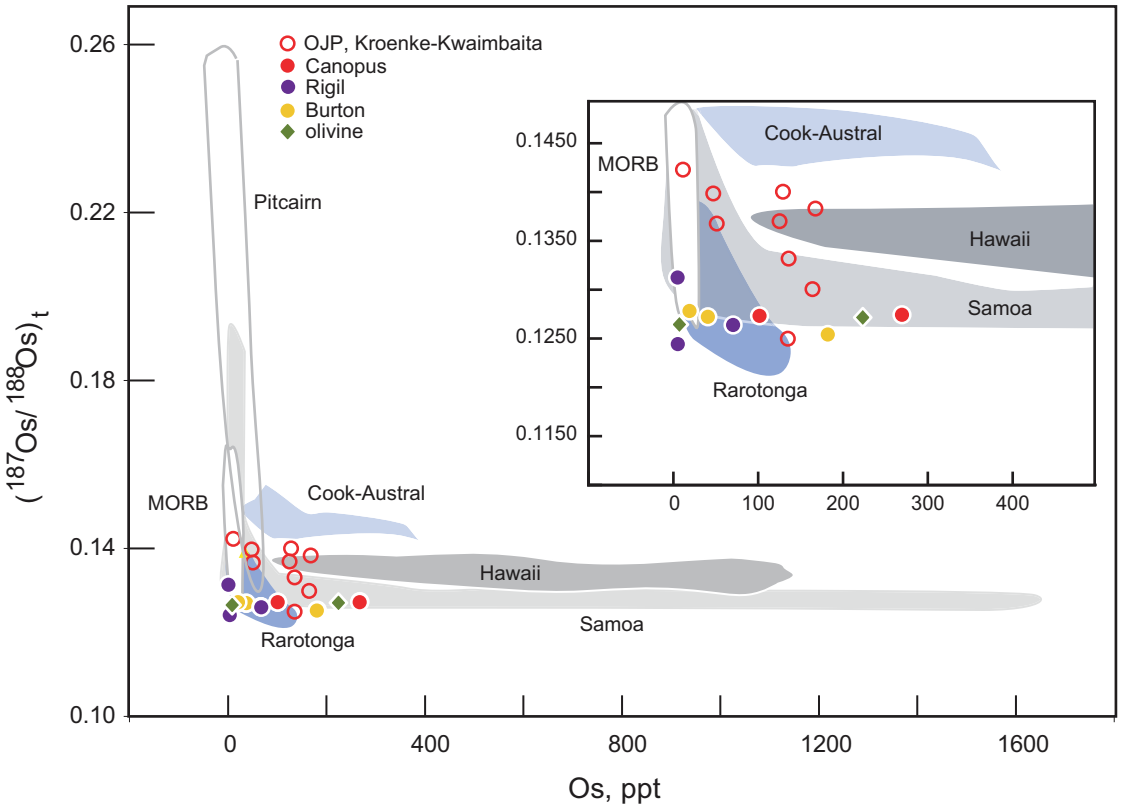

Figure 5. Plot of Os concentration versus Os isotope ratios for LSC basalts (age-corrected) and olivines (present-day) compared with other Pacific ocean island basalts (OIB), mid-ocean ridge basalts (MORB), and Ontong Java Plateau basalts (OJP). The range of Os abundance and isotopic signature of the LSC basalts are relatively limited compared with those of the other Pacific OIBs and overlap with the lower side of the data fields for Samoa and Rarotonga basalts. Data sources are: *Schiano et al.* [1997, 2001]; *Brandon et al.* [1999]; *Eisele et al.* [2002]; *Jackson and Shirey* [2011]; *Hanyu et al.* [2011]; *Tejada et al.* [2013]. Errors are smaller than the symbols.

OIBs range from 0.123 to 0.150 [*Martin*, 1991; *Hauri and Hart*, 1993; *Reisberg et al.*, 1993; *Martin et al.*, 1994; *Roy-Barman and Allegre*, 1995; *Lassiter and Hauri*, 1998; *Brandon et al.*, 1999; *Lassiter et al.*, 2000; *Schiano et al.*, 2001; Eisele et al., 2002; *Gaffney et al.*, 2005; *Bryce et al.*, 2005; *Jamais et al.*, 2008; *Jackson and Shirey*, 2011; *Hanyu et al.*, 2011; *Ireland et al.*, 2011]. The initial Os isotopic values of LSC samples are also mostly lower than those of MORB (0.1277–0.1631) [*Schiano et al.*, 1997]. Among the Pacific OIBs, only Rarotonga (0.1249–0.1285, *Hauri and Hart* [1993]; 0.124–0.139, *Hanyu et al.* [2011]); and Samoa (0.1230–0.1287, *Hauri and Hart* [1993]; 0.1277–0.1313 except for Savai'i, *Jackson and Shirey* [2011]) have comparable Os isotopic compositions with the Louisville samples (Figure 5). All these data, including those of the Louisville basalts, fall between the estimated values for the primitive upper mantle (PUM), with age-corrected $^{187}Os/^{188}Os$ values ranging from 0.1257 to 0.1258 [*Walker et al.*, 2002] and 0.1290 to 0.1291 [*Meisel et al.*, 2001] at 65–77 Ma. These results suggest a dominant mantle signature for the source of the LSC and thus little contribution from the Pacific lithosphere.

Both of the olivine separate samples from Burton seamount have very low Re contents, requiring no age correction and suggesting that their measured $^{187}Os/^{188}Os$ ratios represent those of the Louisville source. The present-day $^{187}Os/^{188}Os$ values for the two olivine samples (0.1272 and 0.1271–0.1275) are in excellent agreement with the age-corrected data for the whole rocks from the same seamount (0.1253–0.1274; Table 2, Figure 5). The olivine data are also identical with the age-corrected values for Canopus seamount basalts (0.1273, 0.1274). These results corroborate previous studies, indicating that olivines indeed preserve pristine magmatic Os isotopic compositions, reflecting those of their source [*Jackson and Shirey*, 2011; *Hanyu et al.*, 2011].

There is no clear correlation between MgO contents and Os and Re concentrations, respectively (Figure 3). High-MgO samples generally possess higher or similar levels of Re concentration compared to Os

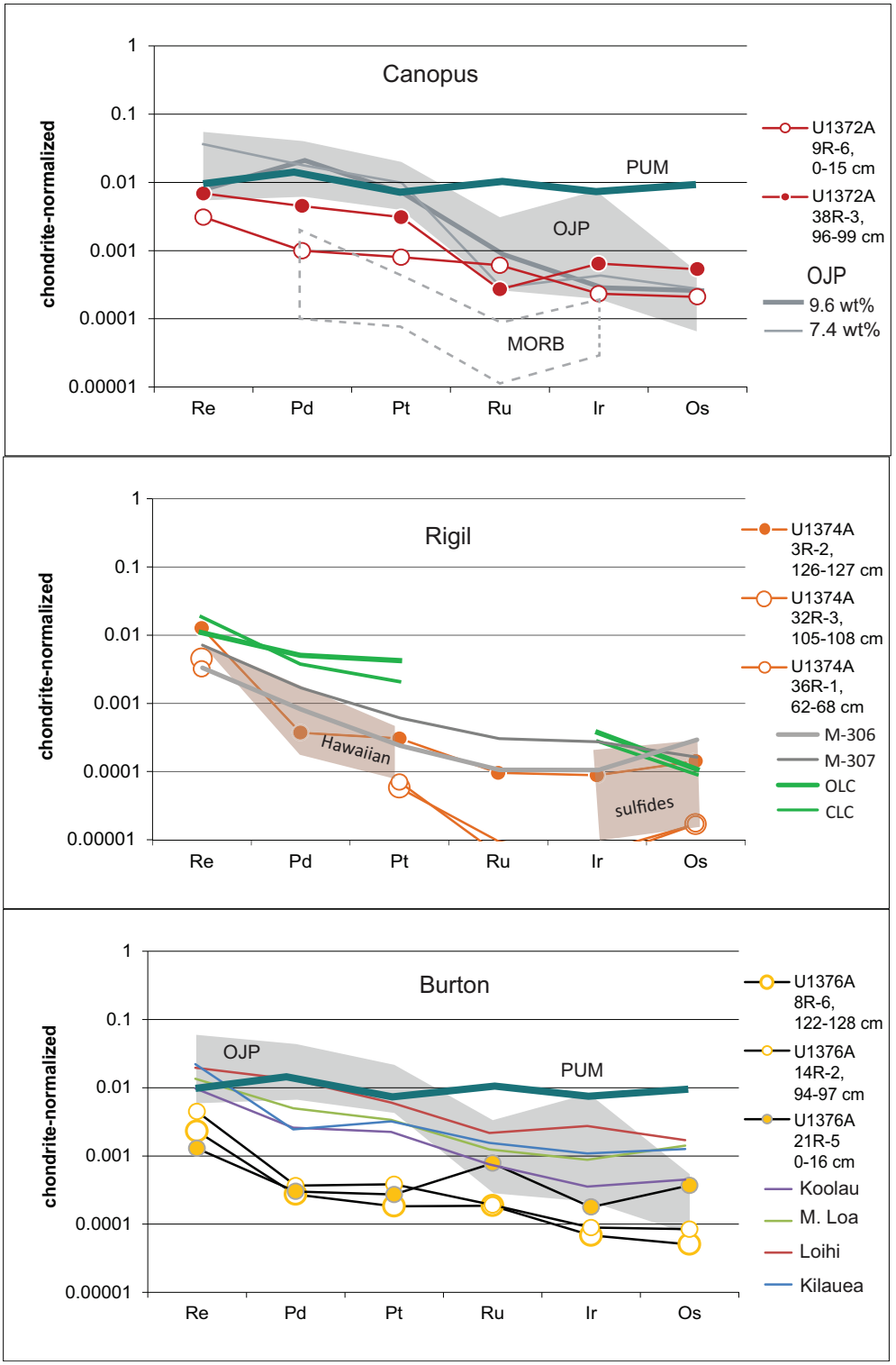

Figure 6. Chondrite-normalized PGE patterns for alkalic and transitional basalts from Canopus, Rigil, and Burton seamounts showing differences in abundance levels and their comparison with Hawaiian picrites [*Bennett et al.*, 2000], Mangaian high-MgO basalts, M-306 and M-307, [*Tatsumi et al.*, 2000; *Hanyu et al.*, 2011], MORB [*Bezos et al.*, 2005], and OJP [*Chazey and Neal*, 2004]. Patterns for primitive upper mantle (PUM) [*Becker et al.*, 2006], oceanic lower crust (OLC), and composite oceanic lower crust (CLC) [*Peucker-Ehrenbrink et al.*, 2003] and Hawaiian included and interstitial sulfides [*Sen et al.*, 2010] are also shown for reference. Normalizing values are from *Palme and Jones* [2003].

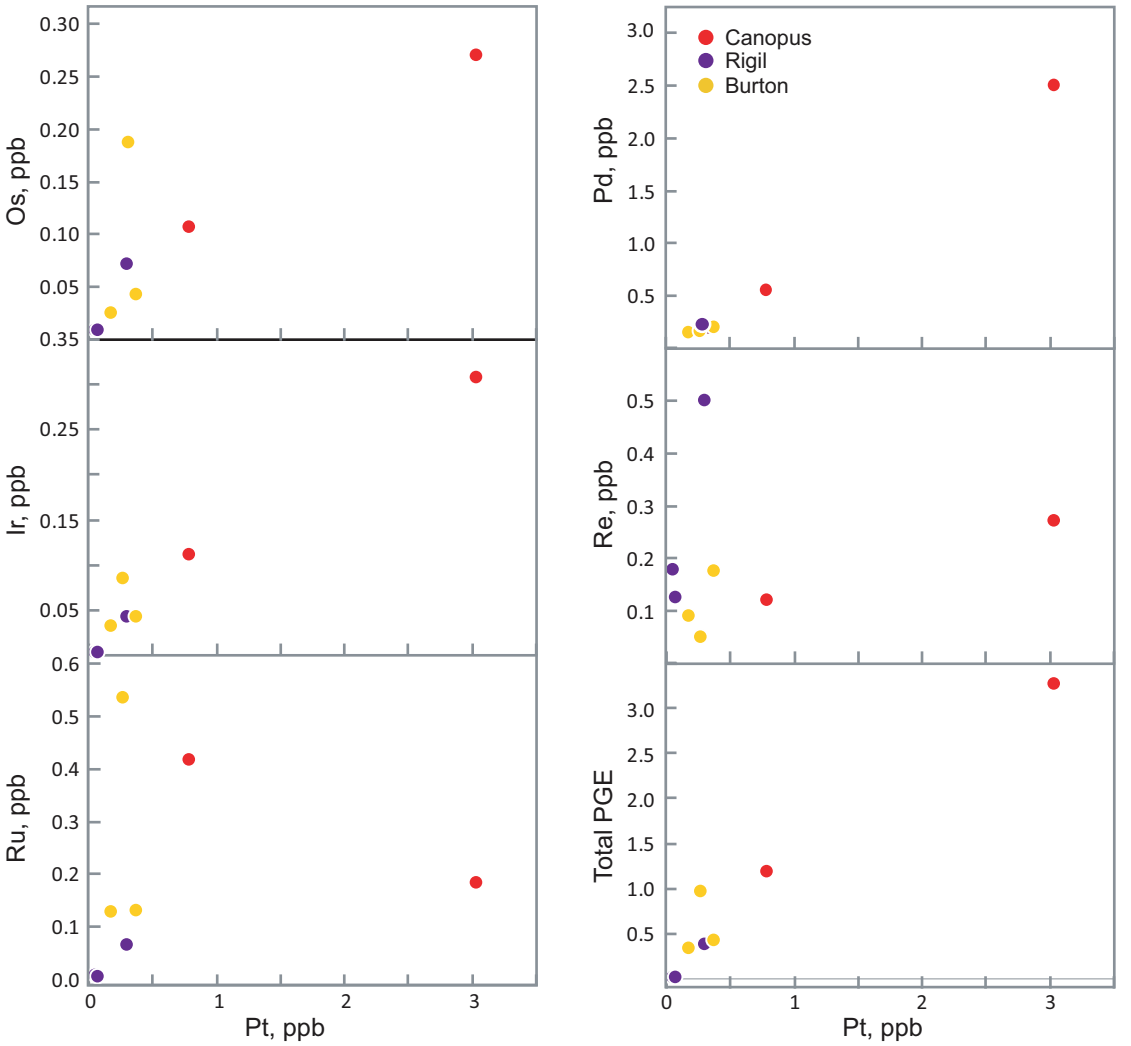

Figure 7. Bivariate plots between other PGEs and total PGE with Pt for Canopus, Rigil, and Burton seamounts basalts showing that they do not correlate with Re and Ru contents.

abundances. However, U1376A-8R-6W, 122–128 cm and U1376-14R-2W, 94–97 cm from Burton seamount have unusually low Os abundances of 26 and 43 ppt, considering their MgO contents of 17 and 13 wt %, respectively (Tables 1 and 2; Figure 3). Interestingly, the Os contents of the olivine separates from these rocks are also highly variable, i.e., they have 231 and 13 ppt, respectively. On the other hand, the low-MgO samples have Re abundances in the same range as those of the high-MgO basalts but lower Os contents. These observations indicate that the Os abundances and isotopic compositions are not controlled by the olivine content of the samples.

4.2. Whole Rock PGE Abundances

The PGE abundances display slight variation between samples within each seamount, e.g., Canopus and Burton, and among seamounts (Figure 6). The Canopus seamount samples have the highest PGE contents, up to one order of magnitude greater than the others. In general, samples from both Canopus and Burton seamounts are similar and have the same gently sloping patterns except for one sample, U1376A 21R-5, 0–16 cm. This sample from Burton seamount displays an almost flat PGE pattern, with chondrite-normalized Pt/Ir and Pd/Ir close to 1, similar to PUM except for the much lower abundance levels. It has the highest MgO content and its porphyritic texture with olivine crystals forming clusters supports its origin through the accumulation of phenocrysts (Figure 3). The rest of the Burton and Canopus samples have Iridium PGE

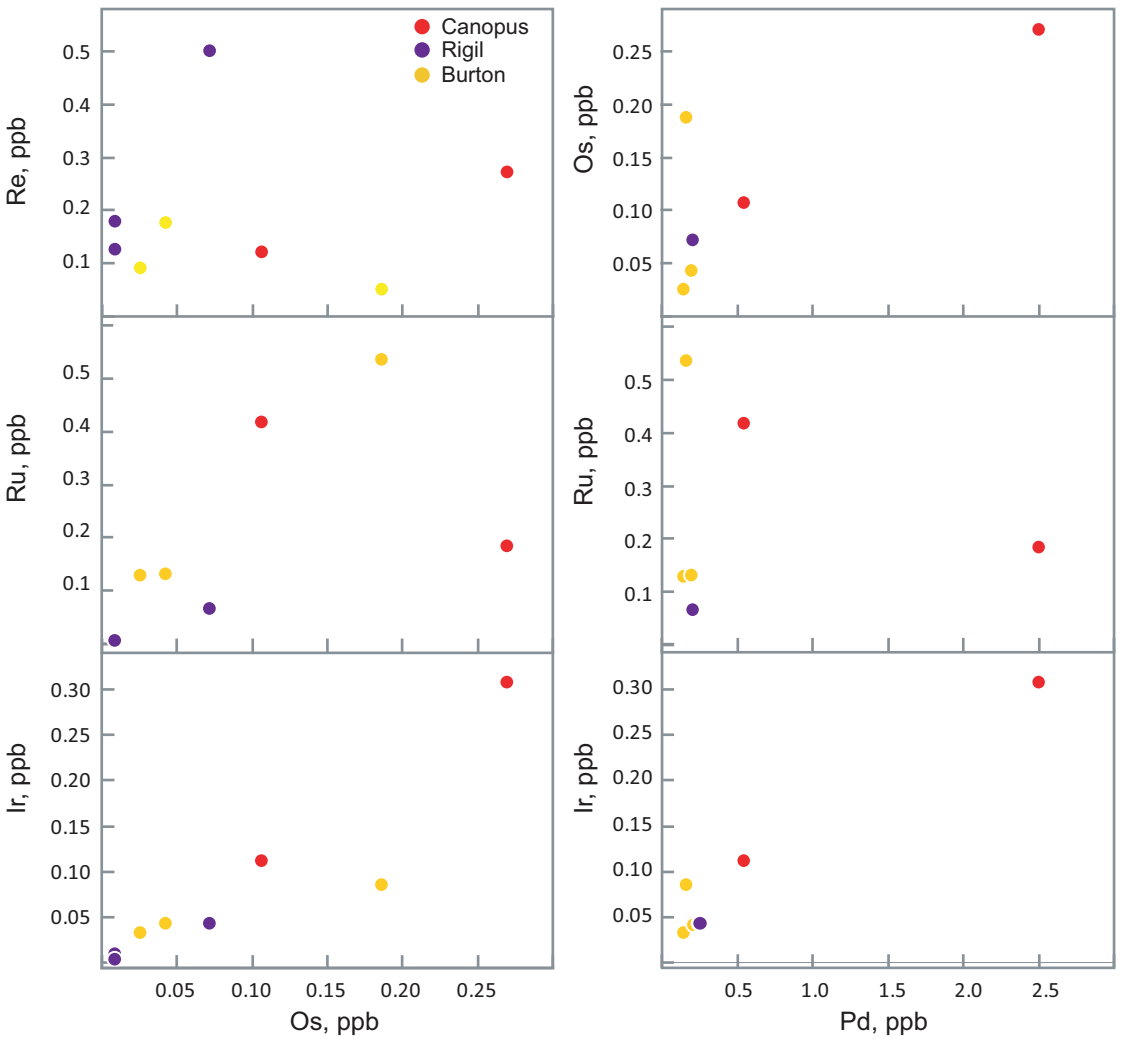

Figure 8. Bivariate plots between other PGEs and Os (first column) and Pd (second column) for Canopus, Rigil, and Burton seamounts basalts showing the absence of correlation with Ru and Re contents.

(Os, Ir, Ru; IPGE) patterns similar to some Hawaiian picrites [*Bennett et al.*, 2000] and OJP basalts [*Chazey and Neal*, 2004] but have markedly lower Platinum PGE contents (Pt, Pd; PPGE, Figure 6). Samples from Rigil seamount have different, slightly concave-up PGE patterns. This type of pattern is found in sulfide inclusions and interstitial sulfides in Hawaiian garnet pyroxenite xenoliths [*Sen et al.*, 2010] and is also shown by alkalic basalts from Mangaia [*Tatsumi et al.*, 2000; *Hanyu et al.*, 2011]. The different PGE patterns may be related to the more alkalic compositions of the Rigil basalts compared to the transitional character of samples from Canopus and Burton seamounts. It is noteworthy that none of the LSC patterns has the same steep slope shown by oceanic lower crust [*Peucker-Ehrenbrink et al.*, 2003], suggesting that this possible lithospheric contaminant has little or no influence on the composition of the Louisville basalts.

Interelement variation plots show that Pt and Pd are well correlated with Os and Ir but not with Re and Ru (Figures 7 and 8). Similarly, total PGE and Pt (and Pd) do not correlate with fractionation indices such as MgO, Ni, and Cr contents (Figure 3) but show some covariation with Cu, except for Burton seamount data (Figure 9). Chondrite-normalized Pt/Ir [$(Pt/Ir)_n = 1.7–4.3$] and Pd/Ir [$(Pd/Ir)_n = 1.5–4.8$] values are modest compared to a large range of 0.5–22.2 and 1.1–19.7 for tholeiites from Kilauea-Iki [*Pitcher et al.*, 2009] and 6.5–65 and 2.8–22, respectively, for OJP [*Chazey and Neal*, 2004] at 9–20 wt % MgO contents. The Louisville data are comparable to those of picrites from Loihi and Mauna Loa (4.8–5.7 and 2.2–3.9) [*Bennett et al.*, 2000] at similar MgO contents but lower than those of Rarotonga (8.2–19.2 and 4.7–9.2) [*Tatsumi et al.*,

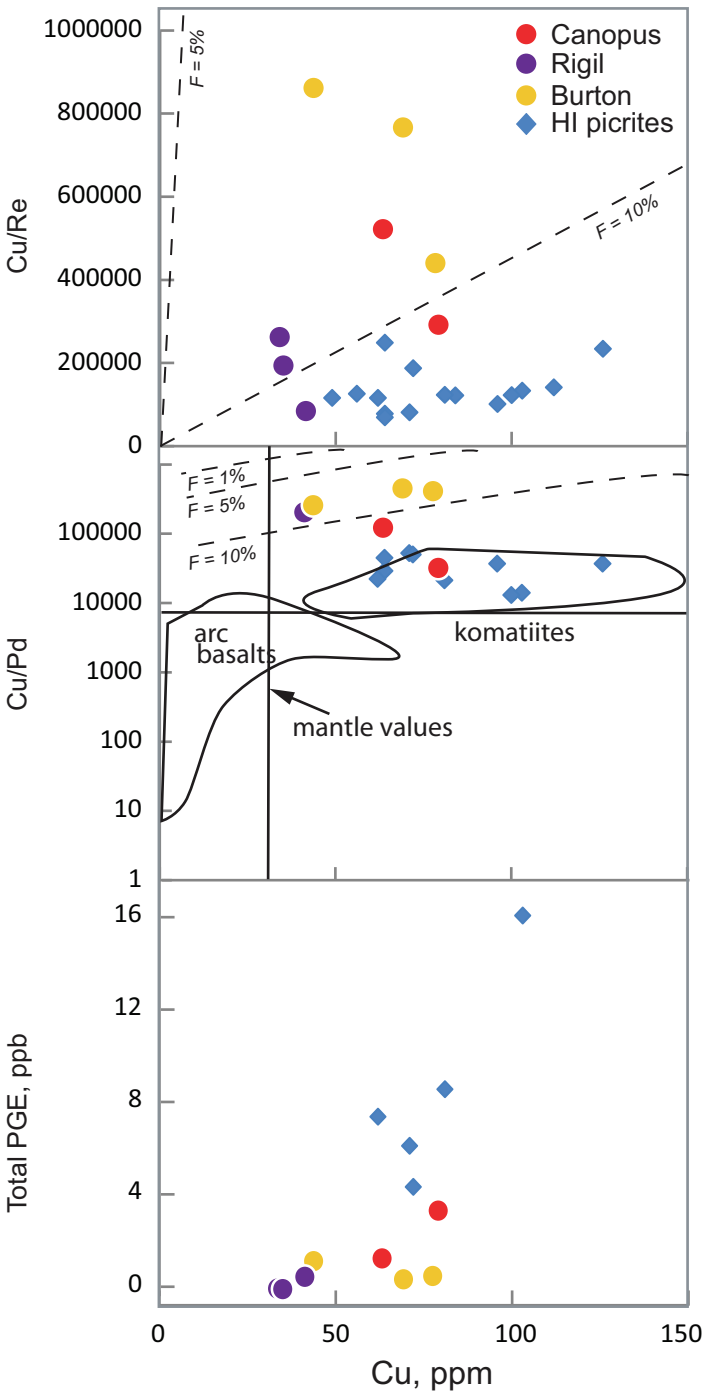

Figure 9. Total PGE, Cu/Pd, and Cu/Re plotted against Cu contents. The higher ratios of LSC basalts can be explained by their lower PGE abundances compared with Hawaiian (HI) picrites, suggesting lower degree of melting under sulfide-saturated condition. Hawaiian picrites data, mantle values and data fields for komatiites and arc basalts are from *Bennett et al.* [2000]. Melting curves are from the modeling results in Figure 10.

2000], Koolau picrites (7.3 and 6.3) [*Bennett et al.*, 2000], and average oceanic lower crust (13.5 and 11.5) [*Peucker-Ehrenbrink et al.*, 2003].

5. Discussion

5.1. Os Isotope Variation and Re-Os Ages

One of the striking characteristics of the LSC is the almost uniform isotopic composition of its volcanic products along the chain [*Cheng et al.*, 1987; *Beier et al.*, 2011; *Vanderkluysen et al.*, 2014], except for the seamounts in the vicinity of the Wishbone Scarp (Figure 1) [*Beier et al.*, 2011]. The limited range in the age-corrected Os isotopic compositions for the Louisville seamount samples compared to other OIBs (Table 2; Figure 5) is in excellent agreement with Pb, Nd, Hf, and Sr isotope data. Some scatter in the data, when compared with the isochrons based on estimated ages (Figure 4a), especially the highest and lowest values for the Rigil seamount samples (Table 2) may be attributed to Re loss or addition during submarine alteration. Furthermore, crustal contamination for samples with low Os contents [*Peucker-Ehrenbrink et al.*, 2003; *Reisberg et al.*, 2008] may also contribute to the scatter in the data. Low, mantle-like age-corrected $^{187}Os/^{188}Os$ values suggest insignificant effect of contamination by the Pacific lithosphere. This may be attributed to the small age difference between the oceanic lithospheric lid and the Louisville seamounts ($\leq$30 Myrs) [*Lonsdale*, 1988], such that the Os isotopic composition of the contaminant was very close to that of the Louisville magma when they were erupted.

Rhenium loss, leading to an insufficient age-correction and thus a higher than expected initial $^{187}Os/^{188}Os$ ratio based on olivine data, may have been caused by shallow submarine to subaerial degassing [*Lassiter*, 2003] as most of the drilled LSC lavas were degassed [*Nichols et al.*, 2014]. On the other hand, Re gain during submarine alteration would have led to too much of an age correction for some Rigil and Burton seamounts

data that plot off the isochron lines, leading to much lower than expected initial $^{187}Os/^{188}Os$ ratios indicated by the olivine data (Table 2). Magnified examination of crushed fragments for samples U1374 36R-1, 62–68 cm and 32R-3, 105–108 cm showed some hair-fine veinlets ($\leq$1 mm wide) and slight brownish alteration of olivine, suggesting that they have suffered alteration that may have not been completely removed by picking. Another sample, U1374-52R-2, 96–99 cm, is finely vesicular and contains very fine amygdules that may have not been totally avoided during the sample preparation, resulting in anomalously very high Os isotopic ratios, which are not reported in Table 2. The phenocryst-enriched sample from Burton seamount, U1376-21R-5, 0–16 cm may have also experienced some Re gain from submarine alteration as indicated by its higher LOI value (5.4 wt %) relative to others. Nevertheless, most of the altered parts may have been avoided during sample preparation or alteration may have happened shortly after emplacement for most of the samples such that their Os isotopic ratios are very close to magmatic values indicated by the data for the olivine separates. Note that most of the data plot along their respective isochrons, considering the errors in $^{187}Re/^{188}Os$ ratios, suggesting that Re loss or gain was insignificant (Figure 4). Furthermore, the initial Os isotope ratios obtained for the Canopus and Burton seamounts samples are remarkably similar to those measured for the olivine separates, suggesting the reliability of these data.

Using the robust regression model of *Ludwig* [2003] gives an isochron age of 71 $+9.7/-15$ Ma and an initial $^{187}Os/^{188}Os$ ratio of 0.127 $\pm$ 0.015 for the Rigil seamount data (Figure 4a). Interestingly, both Canopus and Rigil seamounts data fall along the 72 Ma isochron line, giving an apparent age of 72 $\pm$ 2.8 Ma and an initial $^{187}Os/^{188}Os$ value of 0.1278 $\pm$ 0.0004, suggesting that these two seamounts may have been formed within a short-time interval (Figure 4a). Indeed, the Canopus and Rigil seamounts are believed to have been formed within only a few million years of each other (Site U1372, 74.2 $\pm$ 0.5 Ma; Site U1374, 70.7 $\pm$ 0.6 Ma) [*Koppers et al*., 2012a, 2012b]. In contrast, the Burton seamount data plot along a 65 Ma isochron, consistent with its younger ^{40}Ar-^{39}Ar age [*Koppers et al*., 2012b], except for that of sample U1376-21R-5, 0–16 cm (Figure 4a). Excluding this sample with possible Re gain effect, plotting to the right of the 65 Ma isochron, the whole rock and olivine data for Burton seamount define an isochron age of 64.9 $\pm$ 3.2 Ma and an initial $^{187}Os/^{188}Os$ value of 0.1272 $\pm$ 0.0008 (Figure 4b). These Re-Os ages are very close to the ^{40}Ar-^{39}Ar data for Site U1376 (64.1 $\pm$ 0.5 Ma) [*Koppers et al*., 2012a, 2012b]. The agreement between Re-Os ages and available ^{40}Ar-^{39}Ar data further indicates that the Re-Os data for these samples are not significantly disturbed by alteration or contamination. In addition, the initial $^{187}Os/^{188}Os$ ratios obtained from the isochrons are identical to those of the olivine separates, which likely represent the original magmatic composition and that of the LSC mantle source.

5.2. Controls on PGE Variation

Although the Os isotope compositions do not show any significant difference along the chain from Canopus to Burton seamount, there are obvious variations in the relative and absolute abundance of PGE among the three seamounts. These differences may reflect magmatic processes that control the behavior of the PGE, such as magmatic differentiation and partial melting of the same mantle source. *Pitcher et al*. [2009] have shown that PGE concentrations vary with fractionation of olivine and chromite in the Kilauea Iki lavas (Figure 3). However, this fractionation effect is not displayed by the picrites and tholeiites from different Hawaiian islands [*Tatsumi et al*., 1999; *Bennett et al*., 2000]. The same is true for the different Louisville seamount samples, as shown by plots of PGE versus MgO contents, although olivine fractionation is evident from the tight correlation among MgO, Ni, and Cr (Figure 3). Instead, total PGE, Pt, and Pd show better correlation with Cu (Figure 9). Cu and PGE are all chalcophile elements and behave as incompatible elements in sulfide-undersaturated melts [e.g., *Barnes and Picard*, 1993]. In addition, PGE have higher partition coefficients in sulfides than that of Cu [*Fleet et al*., 1996]. Thus, the correlation of Cu with PGE may be used to assess the role of sulfides in controlling the PGE abundance in the Louisville basalts.

Ratios of Cu with Pd and Re are much higher in Louisville samples than in Hawaiian picrites (Figure 9). The constant and higher than mantle Cu/Pd ratios in Hawaiian picrites are interpreted to be an indication of residual sulfide in their source [*Bennett et al*., 2000]. Because Cu contents are not so different between the Hawaiian picrites and Louisville basalts, this may be explained by the lower concentrations of Re and PGEs in the latter (Figure 3). Consequently, the Cu/Pd ratios in Louisville basalts could indicate residual sulfide in their source and that the much higher ratios result from lower degree of melting (2–7% [*Vanderkluysen et al*., 2014] versus 5–10% for Hawaiian picrites [*Norman and Garcia*, 1999]), assuming the same amounts of sulfides in their source. Thus, it follows that the high-MgO basalts from Canopus and Burton seamounts

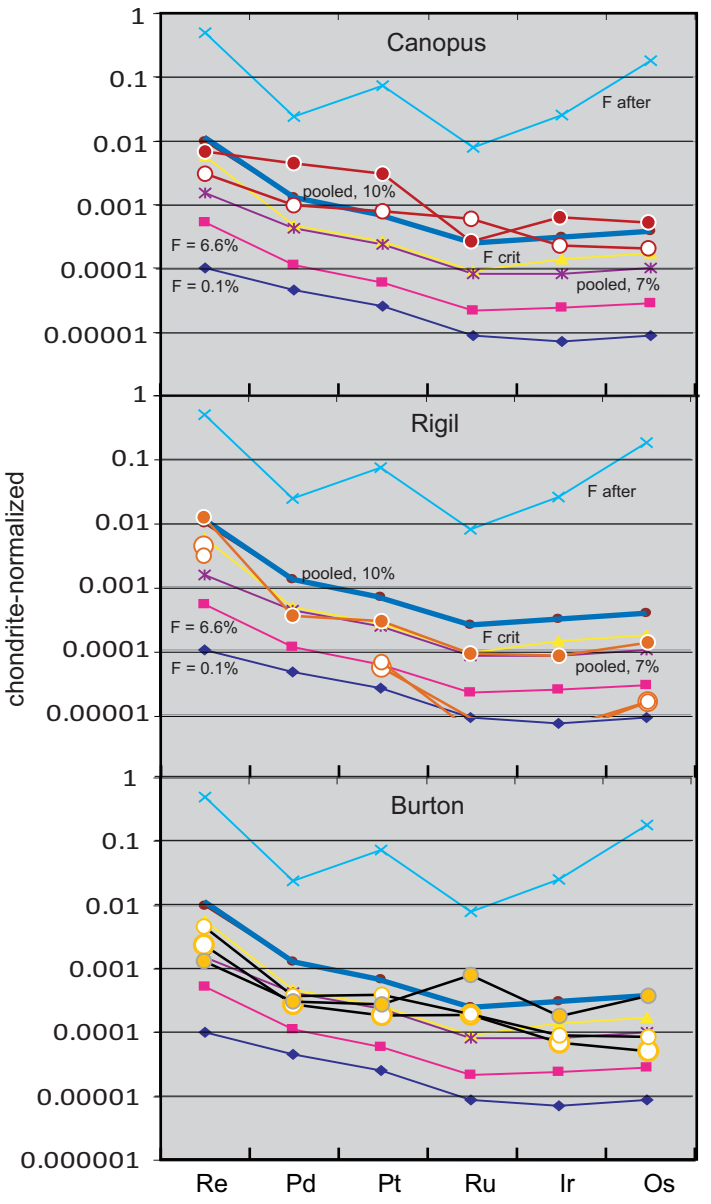

Figure 10. Comparison of fractional melting model-derived PGE abundances with the PGE patterns of LSC basalts. The variation in the LSC patterns can be explained by variable low degree melting of a relatively fertile mantle with 0.015 modal wt % sulfides (range for lherzolites is 0.01–0.03 wt % [*Luguet et al.*, 2003]). Starting PGE composition was assumed to be similar to primitive mantle (Re = 35 ppb, Pd = 7.1 ppb, Pt = 7.6 ppb, Ru = 7 ppb, Ir = 3.5 ppb, and Os = 3.9 ppb) [*Becker et al.*, 2006; *Fischer-Gödde et al.*, 2011] although the best fit models were attained with a lower Re initial content (30 ppb). Melting model and partition coefficients followed those of *Mungall and Brenan* [2014]. Results are shown for the instantaneous initial and sixth fractional melting steps (F = 0.1% and F = 6.6%, respectively), pooled melts from F = 1–6.6% and F = 1–9.9% and right before (F crit, at 9.9%) and after (F after, at 11%) sulfide exhaustion. See text for further details of the melting model.

may have been products of higher degrees of melting compared to that responsible for the lower-MgO Burton and Rigil seamount basalts. Comparison with the relative PGE abundances in model melts produced at different degrees of melting [*Mungall and Brenan*, 2014] suggests that the variation in PGE patterns among Louisville samples may be controlled by partial melting under sulfide-saturated conditions.

A melting model, following the fractional melting simulation by a series of very small degree batch melting calculations [*Mungall and Brenan*, 2014], shows that the PGE abundance patterns of samples from Canopus, Burton, and Rigil can be explained by variable degrees of melting of the same PUM-like source (see Figure 10 caption for PGE composition). The modeling assumes 1.1 wt % increments of batch partial melting calculations, with only the excess 0.1 wt % fraction of every batch melting step pooled together and the remaining amount combined with the restite to form the starting composition of the next batch melting step. The addition of the resulting PGE contents from each batch melting step back to the starting composition simulates the retention of partial melts along grain boundaries in the source [*Mungall and Brenan*, 2014]. The 0.1% partial melt fractions from each melting step were combined together with equal weights to represent the pooled melts. This way of combining melt fractions assumes a columnar melting model as suggested for hotspots and melting above plume heads [*Mungall and Brenan*, 2014].

The best fit results show that the Rigil and the Burton patterns with lower PGE contents may be reproduced by the composition of pooled melts from 1 to 6.6% partial melting increments of a PUM-like mantle source [*Becker et al.*, 2006; *Fischer-Godde et al.*, 2011] with ~0.015 wt % modal residual sulfide (Figure 10). The

amount of modal residual sulfide required by the model is within the range determined for lherzolites (0.01–0.03 wt %) [*Luguet et al*., 2003]. The higher PGE abundances of the high-MgO Canopus and Burton basalts require a larger amount of pooled melts from a longer melting column or a greater number of partial melting increments (F = 1–9.9%) of the same source, just before sulfide exhaustion (at F = 11%). In addition, the PGE abundance in the high-MgO Canopus sample may also indicate fractionation of olivine, without accompanying sulfide saturation. Alternatively, mixing with extremely low amounts of partial melts after sulfide exhaustion may also lead to higher Os, Ir, Pt, and Pd contents and lower Ru content (Figure 10). In contrast, the more evolved nature of the Rigil seamount samples with the lowest PGE contents indicate the possibility that sulfide saturation was reached during olivine crystallization, leading to the fractionation of sulfides and lower PGE contents. Olivine crystallization may lead to sulfide precipitation by producing sulfide saturation in the melt [*Burton et al*., 2002]. This is evident from the lower Cu and Ni contents of the Rigil basalts compared to Burton and Canopus samples and the low Cu contents in most fractionated glasses from the same seamount, suggesting that the melts could have been saturated with an immiscible sulfide phase [*Nichols et al*., 2014].

5.3. The Nature of the LSC Source

The limited isotopic composition of the dredged samples available so far stands witness to the remarkable homogeneity of the LSC mantle source [*Cheng et al*., 1987; *Hawkins et al*., 1987; *Beier et al*., 2011; *Vanderkluysen et al*., 2014]. This is made even more significant by the fact that these basalts are products of low-degree melting, indicating that they are sampling a pure signature of their mantle source. This means either that this mantle source is not diluted or mixed with those of other potential source components (in the case where the scale of melting is larger than those of source components) or that this mantle source is larger in scale than the degree of melting. Given that a number of OIBs appear to sample this mantle source, and the low estimated degree of melting for LSC [*Vanderkluysen et al*., 2014], the latter case is more likely. An average age-corrected $^{187}Os/^{188}Os$ ratio of 0.1271 ± 0.0007 and the range of initial $^{187}Os/^{188}Os$ = 0.1263–0.1274 (except for three ratios compromised by alteration) falls between the two estimated ranges of primitive mantle values of 0.1290–0.1291 [*Meisel et al*., 2001] and 0.1257–0.1258 [*Walker et al*., 2002] at 64–74 Ma and suggest that the source of the Louisville basalts is dominantly oceanic mantle, with no or insignificant contribution from the Pacific lithosphere or deeply recycled crust inferred for most OIBs (Figure 5). It is notable that, unlike those Mangaian basalts whose high $^{187}Os/^{188}Os$ ratios are attributed to recycled crust in their source, the Pt, Pd, and Ir contents of the LSC basalts are lower and Os concentrations higher compared to oceanic lower crustal composition (Figure 6). Moreover, the range of initial $^{187}Os/^{188}Os$ ratios for the LSC seamounts is much smaller and mostly lower than MORB (0.1277–0.1631) [*Schiano et al*., 1997] These results, together with published Pb, Nd, and Sr isotope data, suggest that LSC mantle could indeed represent a distinct mantle source. What then is the nature of the LSC mantle source?

If the Louisville basalts indeed originate from the so-called FOZO mantle, then their Os isotope composition is consistent with the interpretation that they represent the common, possibly fed from the deep, lower mantle sampled by many OIBs [*Hart et al*., 1992; *Hanan and Graham*, 1996; *Lee et al*., 2010]. It is noteworthy that the Os isotopic composition of the basalts from Ofu Island in the Samoan hotspot chain, with similar FOZO- or primitive He mantle (PHEM) [*Farley et al*., 1992] source signature, is just slightly higher (0.1279–0.1294 [*Jackson and Shirey*, 2011]) compared to those of the LSC basalts. These Samoan basalts also possess the highest $^{3}He/^{4}He$ ratios (19.5–33.8 Ra) in the southern hemisphere and exhibit slight variation in their $^{87}Sr/^{86}Sr$ (0.704438–0.704795), $^{143}Nd/^{144}Nd$ (0.512800–0.512844), and $^{206}Pb/^{204}Pb$ (19.126–19.257) [*Jackson et al*., 2007]. Such characteristics are in good agreement with the primordial Ne isotope signature ($^{20}Ne/^{22}Ne$ = 9.8–10.3) and the slightly elevated $^{3}He/^{4}He$ signature ($^{3}He/^{4}He$ = 8.8–10.6 Ra), relative to normal MORB, obtained from the same samples from this study [*Hanyu*, 2014], as well as the limited Sr-Nd-Pb isotopic compositions ($(^{87}Sr/^{86}Sr)_t$ = 0.70285–0.70398; $(^{143}Nd/^{144}Nd)_t$ = 0.512814–0.512864; $(^{206}Pb/^{204}Pb)_t$ = 19.060–19.385; *Cheng et al*. [1987]; *Hawkins et al*. [1987]; *Beier et al*. [2011]; *Vanderkluysen et al*. [2014]) of most LSC basalts. Thus, the evidence available so far points to the existence of a near-primitive mantle that is possibly tapped by both LSC and Ofu Island basalts. Recycled components lead to higher $^{187}Os/^{188}Os$ values observed for other Samoan and Rarotongan basalts but appear to have no significant effect on the LSC composition. Combined with the gently sloping PGE patterns negating oceanic lower crust influence, the limited range of LSC Os isotopic data do not support the suggestion that FOZO represents a well-stirred mixture of recycled oceanic crust [*Kellogg et al*., 2004; *Stracke et al*., 2005]. Such mixture

would be expected to have steeply sloping PGE patterns and radiogenic $^{187}Os/^{188}Os$ of at least 0.146 that would increase with age [*Peucker-Ehrenbrink et al*., 2003, 2012].

The Re-Os isotope system is an excellent tracer of recycled crustal materials because these possess high Re/Os that develop radiogenic Os isotope compositions over time, making their presence easily traceable. Contamination or mixing of recycled crustal material could lead to dilutional effects on mantle PGE and push Os isotopic compositions to more radiogenic values [*Day*, 2013]. Note that, in the case of LSC samples, there is no significant difference in $^{187}Os/^{188}Os$ ratios between low PGE samples from Rigil and Burton seamounts and the high PGE basalts from Canopus seamount (Tables 1 and 2). In contrast, the OJP tholeiites, inferred to originate from a well-homogenized mantle source considering the large (20–30%) degrees of melting [e.g., *Fitton and Godard*, 2004] and the limited range in Pb, Nd, Sr isotope composition [*Mahoney et al*., 1993; *Tejada et al*., 1996, 2002, 2004], show recycled material influence on their Os isotopic ratios [*Tejada et al*., 2013]. Both OJP and Hawaiian high-MgO basalts are suggested to contain up to 28% recycled crust [*Sobolev et al*., 2005, 2007]. If true, this is possibly the reason why both have elevated $^{187}Os/^{188}Os$ and steeper sloping PGE patterns compared to LSC and Samoan basalts (Figure 5).

5.4. Relationship With OJP

The link between the LSC and OJP mantle source hangs on a very thin thread based on available isotopic composition [*Mahoney and Spencer*, 1991; *Vanderkluysen et al*., 2014]. Our present Os isotope and PGE results are also not favorable to a linkage between LSC and OJP. Both the Os isotopic composition and PGE abundance patterns of the OJP tholeiites are more comparable to those of Hawaiian basalts (Figures 5 and 6) [*Tejada et al*., 2013; *Chazey and Neal*, 2004], consistent with their lithophile element isotopic composition, and quite different from those of the LSC. However, younger alkalic volcanism on the OJP may indicate some heterogeneity associated with the plateau's source, if they represent the later stages of its plume head to tail hotspot development [*Tejada et al*., 2015]. Most of these younger alkalic rocks possess similar to higher $^{206}Pb/^{204}Pb$ ratios than those of OJP tholeiites and one group, the ~90 Ma Sigana Alkalic Suite, even exhibit HIMU-like Pb isotopic composition [*Tejada et al*., 1996]. With this consideration, it is still possible that the LSC mantle source could be present in the source of the OJP and warrants further exploration in the future.

6. Conclusions

Re-Os isotope and PGE data obtained from the LSC basalts give better insight into the nature of the so-called Focal Zone mantle sampled by many OIBs and sulfide control on magmatic processes. The range of initial $^{187}Os/^{188}Os$ ratios is small and falls well within the two estimated values for PUM, ruling out significant recycled components in the LSC source. Re-Os isochron ages of 72 ± 2.8 Ma for the older Canopus and Rigil seamounts and 64.9 ± 3.2 Ma for the younger Burton seamount are in excellent agreement with ^{40}Ar-^{39}Ar data. Isochron-derived initial $^{187}Os/^{188}Os$ (0.1272) is also identical to that obtained from olivine separates and likely represents that of the LSC mantle source. The PGE abundances in the LSC basalts are unlike those of oceanic lower crust and the best fit results from modeling require a relatively fertile mantle source. Slight variation in the PGE contents of LSC basalts is best explained by variable low-degree melting in the presence of residual sulfides. These results, together with limited range in lithophile element and primordial noble gas isotope data, could represent the portrait of a deeply-rooted mantle source tapped by the LSC basalts and some Polynesian OIBs. Such mantle may be present in the source of the OJP but is not discernible in the composition of the main-phase plateau basalts.

Acknowledgments

All the data used in this paper are included in Tables 1 and 2. Complete major and trace element data can be requested from G. Fitton and R. Williams. This research used samples provided by the Integrated Ocean Drilling Program (IODP) collected during IODP Expedition 330 by T. Hanyu. We thank the Captain and commend the incredible skill and effort of the crew of JOIDES Resolution in recovering these drill samples. Y. Otsuki is appreciated for her assistance with the analytical work. The paper benefited from discussions with A. R. L. Nichols and the very detailed and critical comments and suggestions of A. A. P. Koppers, C. Beier, and L. Vanderkluysen. We also thank J. Blichert-Toft for her editorial handling of the paper. This paper is dedicated to the memory of late Professor John Mahoney, a highly regarded mentor, friend, and who was also one of the Expedition 330 Scientists.

References

Barnes, S-J., and C. P. Picard (1993), The behavior of platinum-group elements during partial melting, crystal fractionation, and sulphides segregation: An example from the Cape Smith Fold Belt, northern Quebec, *Geochim. Cosmochim. Acta*, *57*, 79–87.

Becker, H., M. F. Horan, R. J. Walker, S. Gao, J.-P., Lorand, R. L. Rudnick (2006), Highly siderophile element composition of the Earth's primitive upper mantle: Constraints from new data on peridotite massifs and xenoliths, *Geochim. Cosmochim. Acta*, *70*, 4528–4550.

Beier, C., L. Vanderkluysen, M. Regelous, J. J. Mahoney, and D. Garbe-Schönberg (2011), Lithospheric control on geochemical composition along the Louisville Seamount Chain, *Geochem. Geophys. Geosyst.*, *12*, Q0AM01, doi:10.1029/2011GC003690.

Bennett, V. C., M. D. Norman, and M. O. Garcia (2000), Rhenium and platinum group element abundances correlated with mantle source components in Hawaiian picrites: Sulphides in the plume, *Earth. Planet. Sci. Lett.*, *183*, 513–526.

Bezos, A., J.-P. Lorand, E. Humler, and M. Gros (2005), Platinum-group element systematics in Mid-Oceanic Ridge basaltic glasses from the Pacific, Atlantic, and Indian Oceans, *Geochim. Cosmochim. Acta*, *69*, 2613–2627.

Brandon, A. D., M. D. Norman, R. J. Walker, and J. W. Morgan (1999), ^{186}Os-^{187}Os systematics of Hawaiian picrites, *Earth Planet. Sci. Lett.*, *174*, 25–42.

Bryce, J. G., D. J. DePaolo, and J. C. Lassiter (2005), Geochemical structure of the Hawaiian plume: Sr, Nd, and Os isotopes in the 2.8 km HSDP-2 section of Mauna Kea volcano, *Geochem. Geophys. Geosyst.*, *6*, Q09G18, doi:10.1029/2004GC000809.

Burton, K. W., A. Gannoun, J.-L., Birck, C. J. Allegre, P. Schiano, R. Clocchiatti, and O. Alard (2002), The compatibility of rhenium and osmium in natural olivine and their behavior during mantle melting and basalt genesis, *Earth Planet. Sci. Lett.*, *198*, 63–76.

Chazey, W. J., and C. R. Neal (2004), Large igneous province magma petrogenesis from source to surface: Platinum-group element evidence from Ontong Java Plateau basalts recovered during ODP Legs 130 and 192, in *Origin and Evolution of the Ontong Java Plateau, Spec. Publ. 229*, edited by Fitton, J. G. et al., pp. 219–238, Geol. Soc. London, London, U. K.

Cheng, Q., K.-H. Park, J. D. Macdougall, A. Zindler, G. W. Lugmair, H. Staudigel, J. Hawkins, and P. Lonsdale (1987), Isotopic evidence for a hotspot origin of the Louisville seamount chain, in *Seamounts, Islands, and Atolls, Geophys. Monogr. Ser. 43*, edited by B. H. Keating et al., pp. 283–296, AGU, Washington, D. C.

Cohen, R. S., and F. G. Waters (1996), Separation of osmium from geological materials by solvent extraction for analysis by thermal ionization mass spectrometry, *Anal. Chim. Acta*, *332*, 269–275.

Courtillot, V., A. Davaille, J. Besse, and J. Stock (2003), Three distinct types of hotspots in the Earth's mantle, *Earth Planet. Sci. Lett.*, *205*, 295–308, doi:10.1016/S0012–821X(02)01048-8.

Dale, C. W., C. G., Macpherson, D. G. Pearson, S. J., Hammond, and R. J. Arculus (2012), Inter-element fractionation of highly siderophile elements in the Tonga Arc due to flux melting of a depleted source, *Geochim. Cosmochim. Acta*, *89*, 202–225.

Day, J. M.D. (2013), Hotspot volcanism and highly siderophile elements, *Chem. Geol.*, *341*, 50–74.

Eisele, J., M. Sharma, S. J. G. Galer, J. Blichert-Toft, C. W. Devey, and A. W. Hoffman (2002), The role of sediment recycling in EM-1 inferred from Os, Pb, Hf, Nd, Sr isotope and trace element systematics of the Pitcairn hotspot, *Earth Planet Sci. Lett.*, *196*, 197–212.

Expedition 330 Scientists (2011), Louisville Seamount Trail: Implications for geodynamic mantle flow models and the geochemical evolution of primary hotspots, in *Integr. Ocean Drill. Program Prelim. Rep. 330*, Integr. Ocean Drill. Program Manage. Int., Inc., Tokyo, Japan, doi:10.2204/iodp.pr.330.2011.

Farley, K. A., J. H. Natland, and H. Craig (1992), Binary mixing of enriched and undegassed (primitive?) mantle components (He, Sr, Nd, Pb) in Samoan lavas, *Earth Planet. Sci. Lett.*, *111*, 183–199.

Fischer-Gödde, M., H. Becker, and F. Wombacher (2011), Rhodium, gold and other highly siderophile elements in orogenic peridotites and peridotite xenoliths, *Chem. Geol.*, *280*, 365–383.

Fitton, J. G., and M. Godard (2004), Origin and evolution of magmas on the Ontong Java Plateau, in *Origin and Evolution of the Ontong Java Plateau, Geological Society, London, Spec. Publ. 229*, edited by J. G. Fitton et al., pp. 151–178, Geol. Soc. London, London, U. K.

Fitton, J. G., A. D. Saunders, L. M. Larsen, B. S. Hardarson, and M. J. Norry (1998), Volcanic rocks from the southeast Greenland margin at 63°N: Composition, petrogenesis and mantle sources, *Proc Ocean Drill. Program, Sci. Results*, *152*, 331–350.

Fleet, M. E., J. H. Crocket, and W. E. Stone (1996), Partitioning of platinum group elements (Os, Ir, Ru, Pt, Pd) and gold between sulphides liquid and basalt melt, *Geochim. Cosmochim. Acta*, *60*, 2397–2412.

Gaffney, A. M., B. K. Nelson, L. Reisberg, and J. Eiler (2005), Oxygen-osmium isotope systematics of West Maui lavas: A record of shallow-level magmatic processes, *Earth Planet. Sci. Lett.*, *239*, 122–139.

Hanan, B. B., and D. W. Graham (1996), Lead and helium isotope evidence from oceanic basalts for a common deep source of mantle plumes, *Science*, *272*, 991–995.

Hanyu, T. (2014), Deep plume origin of the Louisville hotspot: Noble gas evidence, *Geochem. Geophys. Geosyst.*, *15*, 565–576, doi:10.1002/2013GC005085.

Hanyu, T., et al. (2011), Geochemical characteristics and origin of the HIMU reservoir: A possible mantle plume source in the lower mantle, *Geochem. Geophys. Geosyst.*, *12*, Q0AC09, doi:10.1029/2010GC003252.

Hart, S. R., E. H. Hauri, L. A. Oschmann, and J. A. Whitehead (1992), Mantle plumes and entrainment: Isotopic evidence, *Science*, *256*, 517–520.

Hauri, E. H., and S. R. Hart (1993), Re-Os isotope systematics of HIMU and EMII oceanic island basalts from the south Pacific Ocean, *Earth Planet Sci. Lett.*, *114*, 353–371.

Hawkins, J. W., P. F. Lonsdale, and R. Batiza (1987), Petrologic evolution of the Louisville seamount chain, in *Seamounts, Islands, and Atolls, Geophys. Monogr. Ser. 43*, edited by B. H. Keating, et al., pp. 235–254, AGU, Washington, D. C.

Ireland, T. J., R. J. Walker, and A. D. Brandon (2011), ^{186}Os-^{187}Os systematics of Hawaiian picrites revisited: Insights into Os isotopic variations in ocean island basalts, *Geochim. Cosmochim. Acta*, *75*, 4456–4475.

Ishikawa A., R. Senda, K. Suzuki, C. W. Dale, and T. Meisel (2014), Re-evaluating digestion methods for highly siderophile element and ^{187}Os isotope analysis: Evidence from geological reference materials, *Chem. Geol.*, *384*, 27–46.

Jackson, M. G., and S. B. Shirey (2011), Re-Os isotope systematics in Samoan shield lavas and the use of Os-isotopes in olivine phenocryts to determine primary magmatic compositions, *Earth Planet. Sci. Lett.*, *312*, 191–101.

Jackson, M. G., M. D. Kurz, S. R. Hart, and R. K. Workman (2007), New Samoan lavas from Ofu Island reveal a hemispherically heterogeneous high ^{3}He/^{4}He mantle, *Earth Planet. Sci. Lett.*, *264*, 360–374.

Jamais, M., J. C. Lassiter, G. Brugmann (2008), PGE and Os-isotopic variations in lavas from Kohala Volcano, Hawaii: Constraints on PGE behavior and melt/crust interaction, *Chem. Geol.*, *250*, 16–28.

Kellogg, J. B., S. B. Jacobsen, and R. J. O'Connell (2004), Mantle isotopic heterogeneity: The FOZO's in the pudding, *Eos Trans. AGU*, *85*(17), Jt. Assem. Suppl., Abstract V43A-12.

Koppers, A. A. P., R. A. Duncan, and B. Steinberger (2004), Implications of a nonlinear ^{40}Ar/^{39}Ar age progression along the Louisville seamount trail for models of fixed and moving hot spots, *Geochem. Geophys. Geosyst.*, *5*, Q06L02, doi:10.1029/2003GC000671.

Koppers, A. A. P., M. D. Gowen, L. E. Colwell, J. S. Gee, P. F. Lonsdale, J. J. Mahoney, and R. A. Duncan (2011), New ^{40}Ar/^{39}Ar age progression for the Louisville hot spot trail and implications for inter-hot spot motion, *Geochem. Geophys. Geosyst.*, *12*, Q0AM02, doi:10.1029/2011GC003804.

Koppers, A. A. P., T. Yamazaki, J. Geldmacher, and Expedition 330 Scientists (2012a), Volume 330 expedition reports: Louisville Seamount Trail, in *Proceedings of Integrated Ocean Drilling Program*, Integr. Ocean Drill. Program Manage. Int., Inc., Tokyo, Japan.

Koppers, A. P., et al. (2012b), Limited latitudinal mantle plume motion for the Louisville hotspot, *Nat. Geosci.*, *5*, 911–917.

Lassiter, J. C. (2003), Rhenium volatility in subaerial lavas: Constraints from subaerial and submarine portions of the HSDP-2 Mauna Kea drillcore, *Earth Planet. Sci. Lett.*, *214*, 311–325.

Lassiter, J. C., and E. H. Hauri (1998), Osmium-isotope variations in Hawaiian lavas: Evidence for recycled oceanic lithosphere in the Hawaiian plume, *Earth Planet. Sci. Lett.*, *164*, 483–496.

Lassiter, J. C., E. H. Hauri, P. W. Reiners, and M. O. Garcia (2000), Generation of Hawaiian post- erosional lavas by melting of a mixed lherzolite/pyroxenite source, *Earth Planet. Sci. Lett.*, *178*, 269–284.

Lee, C-T., P. Luffi, T. Hoink, J. Li, R. Dasgupta, and J. Hernlund (2010), Upside-down differentiation and generation of a 'primordial' lower mantle, *Nature*, *463*, 930–935.

Lonsdale, P. (1988), Geography and history of the Louisville hotspot chain in the Southwest Pacific, *J. Geophys. Res.*, *93*(B4), 3078–3104.

Ludwig, K. R. (2003), ISOPLOT 3.00, a geochronological tool kit for Microsoft Excel, *Spec. Publ. vol. 4*, 70 pp., Berkeley Geochronol. Cent., Berkeley, Calif. [Available at http://bgc.org/isoplot_etc/isoplot.html.]

Luguet, A., J.-P. Lorand, and M. Seyler (2003), Sulfide petrology and highly siderophile element geochemistry of abyssal peridotites: A coupled study of samples from the Kane Fracture Zone (45°W 23°20N, MARK Area, Atlantic Ocean), *Geochim. Cosmochim. Acta*, *67*, 1553–1570.

Mahoney, J. J., and K. J. Spencer (1991), Isotopic evidence for the origin of the Manihiki and Ontong Java oceanic plateaus, *Earth Planet. Sci. Lett.*, *104*, 196–210.

Mahoney, J. J. M. Storey, R. A. Duncan, K. J. Spencer, and M. Pringle (1993), Geochemistry and geochronology of the Ontong Java Plateau, in *The Mesozoic Pacific: Geology, Tectonics and Volcanism, Geophys. Monogr. Ser. 77*, edited by M. S. Pringle et al., pp. 233–262, AGU, Washington, D. C.

Martin, C.E. (1991), Osmium isotopic characteristics of mantle-derived rocks, *Geochim. Cosmochim. Acta*, *55*, 1421–1434.

Martin, C. E., R. W. Carlson, S. B. Shirey, F. A. Frey, and C-Y. Chen (1994), Os isotopic variation in basalts from Haleakala Volcano, Maui, Hawaii: A record of magmatic processes in oceanic mantle and crust, *Earth Planet. Sci. Lett.*, *128*, 287–301.

Meisel, T., and J. Moser (2004), Reference materials for geochemical PGE analysis: New analytical data for Ru, Rh, Pd, Os, Ir, Pt and Re by isotope dilution ICP-MS in 11 geological reference materials, *Chem. Geol.*, *208*, 319–338.

Meisel, T., R. J. Walker, A. J. Irving, and J-P. Lorand (2001), Osmium isotopic compositions of mantle xenoliths: A global perspective, *Geochim. Cosmochim. Acta*, *65*, 1311–1323.

Mungall, J. E., and J. M. Brenan (2014), Partitioning of platinum-group elements and Au between sulfide liquid and basalt and the origins of mantle-crust fractionation of the chalcophile elements, *Geochim. Cosmochim. Acta*, *125*, 265–289.

Nichols, A. R. L., C. Beier, P. A. Brandl, D. M. Buchs, and S. H. Krumm (2014), Geochemistry of volcanic glasses from the Louisville Seamount Trail (IODP Expedition 330): Implications for eruption environments and mantle melting, *Geochem. Geophys. Geosyst.*, *15*, 1718–1738, doi:10.1002/2013GC005086.

Norman, M. D., and M. O. Garcia (1999), Primitive magmas and source characteristics of the Hawaiian plume: Petrology and geochemistry of shield picrites, *Earth Planet. Sci. Lett.*, *168*, 27–44.

Palme, J., and A. Jones (2003), Solar system abundances of the elements, in *Treatise on Geochemistry*, vol. 1, pp. 41–61.

Peucker-Ehrenbrink, B., W. Bach, S. R. Hart, J. S. Blusztajn, and T. Abbruzzese (2003), Rhenium- osmium isotope systematics and platinum group element concentrations in oceanic crust from DSDP/ODP Sites 504 and 417/418, *Geochem. Geophys. Geosyst.*, *4* (7), 8911, doi: 10.1029/2002GC000414, 2003.

Peucker-Ehrenbrink, B., K. Hanghoj, T. Atwood, and P. B. Kelemen (2012), Rhenium-osmium isotope systematics and platinum group element concentrations in oceanic crust, *Geology*, *40*, 199–202.

Pitcher, L., R. T. Helz, R. J. Walker, and P. Piccoli (2009), Fractionation of the platinum-group elements and Re during crystallization of basalt in Kilauea Iki Lava Lake, Hawaii, *Chem. Geol.*, *260*, 196–210.

Reisberg, L., A. Zindler, F. Marcantonio, W. White D. Wyman, and B. Weaver (1993), Os isotope systematics in ocean island basalts, *Earth Planet. Sci. Lett.*, *120*, 149–167.

Reisberg, L., O. Rouxel, J. Ludden, H. Staudigel, and C. Zimmermann (2008), Re-Os results from ODP Site 801: Evidence for extensive Re uptake during alteration of oceanic crust, *Chem. Geol.*, *248*, 256–271.

Roy-Barman, M. and C. J. Allegre (1995), $^{187}Os/^{186}Os$ in oceanic island basalts: Tracing oceanic crust recycling in the mantle, *Earth Planet. Sci. Lett.*, *129*, 145–161.

Schiano, P., J.-L. Birck, and C. J. Allegre (1997), Osmium-strontium-neodymium-lead isotopic variations in mid-ocean ridge basalt glasses and the heterogeneity of the upper mantle, *Earth Planet. Sci. Lett.*, *150*, 363–379.

Schiano, P., K. W. Burton, B. Dupre, J.-L. Birck, G. Guille, and C. J. Allegre (2001), Correlated Os-Pb-Nd-Sr isotopes in the Austral-Cook chain basalts: The nature of mantle components in plume sources, *Earth Planet. Sci. Lett.*, *186*, 527–537.

Sen, I. S., M. Bizimis, and G. Sen (2010), Geochemistry of sulfides in Hawaiian garnet pyroxenite xenoliths: Implications for highly siderophile elements in the oceanic mantle, *Chem. Geol.*, *273*, 180–192.

Shinotsuka, K. and K. Suzuki (2007), Simultaneous determination of platinum group elements and rhenium in rock samples using isotope dilution inductively coupled plasma mass spectrometry after cation exchange separation followed by solvent extraction, *Anal. Chim. Acta*, *603*, 129–139.

Sobolev, A. V., A. W. Hoffman, S. V. Sobolev, and I. K. Nikogosian (2005), An olivine-free mantle source of Hawaiian shield basalts, *Nature*, *434*, 590–597.

Sobolev, A. V., et al. (2007), The amount of recycled crust in sources of mantle-derived melts, *Science*, *316*, 412–417.

Stracke, A., A. W. Hofmann, and S. R. Hart (2005), FOZO, HIMU, and the rest of the mantle zoo, *Geochim. Geophys. Geosyst.*, *6*, Q05007, doi: 10.1029/2004GC000824.

Tatsumi, Y., K. Oguri, and G. Shimoda (1999), The behavior of platinum-group elements during magmatic differentiation in Hawaiian tholeiites, *Geochem. J.*, *33*, 237–247.

Tatsumi, Y., K. Oguri, G. Shimoda, T. Kogiso, and H. G. Barsczus (2000), Contrasting behavior of noble metal elements during magmatic differentiation in basalts from the Cook Islands, Polynesia, *Geology*, *28*, 131–134.

Tejada, M. L. G., J. J. Mahoney, R. A. Duncan, and M. P. Hawkins (1996), Age and geochemistry of basement and alkalic rocks of Malaita and Santa Isabel, Solomon Islands, southern margin of Ontong Java Plateau, *J. Petrol.*, *37*, 361–394.

Tejada, M. L. G., J. J. Mahoney, C. R. Neal, R. A. Duncan, and M. G. Petterson (2002), Basement geochemistry and geochronology of Central Malaita, Solomon, Islands, with implications for the origin and evolution of the Ontong Java Plateau, *J. Petrol.*, *43*, 449–484.

Tejada, M. L. G., J. J. Mahoney, P. R. Castillo, S. P. Ingle, H. C. Sheth, and D. Weis (2004), Pin-pricking the elephant: Evidence on the origin of the Ontong Java Plateau from Pb-Sr-Nd-Hf, in *Origin and Evolution of the Ontong Java Plateau, Geological Society, London, Spec. Publ. 229*, edited by J. G. Fitton et al., pp. 133–150, Geol. Soc. London, London, U. K.

Tejada, M. L. G., K. Suzuki, T. Hanyu, J. J. Mahoney, A. Ishikawa, Y. Tatsumi, Q. Chang, and S. Nakai (2013), Cryptic lower crustal signature in the source of the Ontong Java Plateau revealed by Os and Hf isotopes, *Earth Planet. Sci. Lett.*, *377–378*, 84–96.

Tejada M. L. G., et al. (2015), Isotopic evidence for a link between Lyra Basin and Ontong Java Plateau, in *The Origin, Evolution and Environmental Impact of Oceanic Large Igneous Provinces*, edited by C. R. Neal, et al., *Geol. Soc. Am. Spec.*, Paper 511, doi:10.1130/2015.2511(14).

Vanderkluysen, L., J. J. Mahoney, A. A.P. Koppers, C. Beier, M. Regelous, J. S. Gee, and P. F. Lonsdale (2014), Louisville seamount chain: Petrogenetic processes and geochemical evolution of the mantle source, *Geochem. Geophys. Geosyst.*, *15*, 2380–2400, doi:10.1002/2014GC005288.

Walker, R. J., M. F. Horan, J. W. Morgan, H. Becker, J. N. Grossman, and A. E. Rubin (2002), Comparative ^{187}Re-^{187}Os systematics of chondrites: Implications regarding early solar system processes, *Geochim. Cosmochim. Acta*, *66*, 4187–4201.

Watts, A. B., J. K. Weissel, R. A. Duncan, and R. L. Larson (1988), Origin of the Louisville ridge and its relationship to the Eltanin fracture zone system, *J. Geophys. Res.*, *93*(B4), 3051–3077.